Structure and Properties Development in Poly(phenylene sulfide) Fibers, Part I: Effect of Material and Melt Spinning Process Variables

Prabhakar Gulgunje, Gajanan Bhat, Joseph Spruiell

Department of Materials Science and Engineering, The University of Tennessee, Knoxville, Tennesse

Received 4 August 2010; accepted 25 January 2011
DOI 10.1002/app.34353
Published online 7 July 2011 in Wiley Online Library (wileyonlinelibrary.com).

ABSTRACT: The detailed research study of manufacturing PPS fibers using melt spinning and further enhancement of tensile properties by drawing and annealing experiments, a study lacking as of today in open scientific literature, was the focus of this research. This article discusses the effect of polymer molecular weight (MW) and melt spinning process variables on the structure and properties development in melt spun fibers manufactured from proprietary Fortron® linear PPS resins. Structure-properties relationship was studied using several characterization tools like tensile testing, differential scanning calorimetry, polarized light optical microscopy, and wide-angle x-ray scattering. Changes in dynamic mechanical behavior of as-spun fibers manufactured from resins of varying MW and different melt spinning take-up speeds were also studied. The study showed that by a combination of higher MW of the polymer and spinning at higher take-up speeds, tensile properties of as-spun PPS fibers can be improved. © 2011 Wiley Periodicals, Inc. J Appl Polym Sci 122: 3110–3121, 2011

Key words: high performance polymers; thermoplastics; structure-property relations; extrusion; fibers

INTRODUCTION

Since the successful commercial manufacture of high molecular weight (MW) PPS (Ryton® PPS) by Edmonds and Hill[1] at Phillips Petroleum Company in 1960s, it is being used mainly as injection molded plastic in the unfilled, as well as in the compounded form with other fillers like glass fibers for automotive components. The molecular architecture of this PPS was primarily branched or lightly crosslinked.[2,3] Subsequent developments in polymer synthesis made it possible to produce linear grade PPS suitable for extrusion processes, Fortron® being one such material. Due to significant amount of PPS being used to manufacture injection molded components, in the early years, several investigators studied its crystallization kinetics in neat as well as in the filled form.[4–10] Researchers[11–16] reported its susceptibility to chemical changes when exposed to temperatures above its melting point for long durations. Molecular architecture influences the isothermal crystallization kinetics of PPS.[17,18] These studies showed faster nucleation and higher crystallization rates in linear PPS than that in branched PPS. Zhang et al.[19] studied the influence of shear stress on crystallization behavior of PPS, and reported that shear accelerates the formation of stable crystal nuclei by increasing the molecular orientation under shear flow. Therefore, crystallization induction time decreases with shear time.

In comparison to the numerous studies on its crystallization kinetics, very few researchers studied PPS in the fiber form. Song et al.[20] reported melt spinning of Ryton® PPS using the Instron capillary rheometer. It was observed that, with increase in MW of PPS, crystallinity level decreases causing crystalline orientation to drop. That in turn results in decrease in birefringence. Other investigators[21–24] studied draw-annealing of industrially produced PPS as-spun fibers and reported improvement in fiber tensile properties.

The importance of material and fiber manufacturing process variables, including their interaction effects in enhancing the fiber tensile properties in the fibers spun from other thermoplastic polymers, such as polyethylene[25] is well documented in literature. It is apparent that such an understanding of the development of structure and properties in PPS fibers is not investigated, and reported so far, especially for PPS with linear molecular architecture. This research was conducted to elucidate the relationship between polymer MW, and fiber spinning and post processing conditions, on the morphology and properties development in as-spun and draw-annealed PPS

Correspondence to: G. Bhat (gbhat@utk.edu).
Contract grant sponsor: Ticona Polymers.

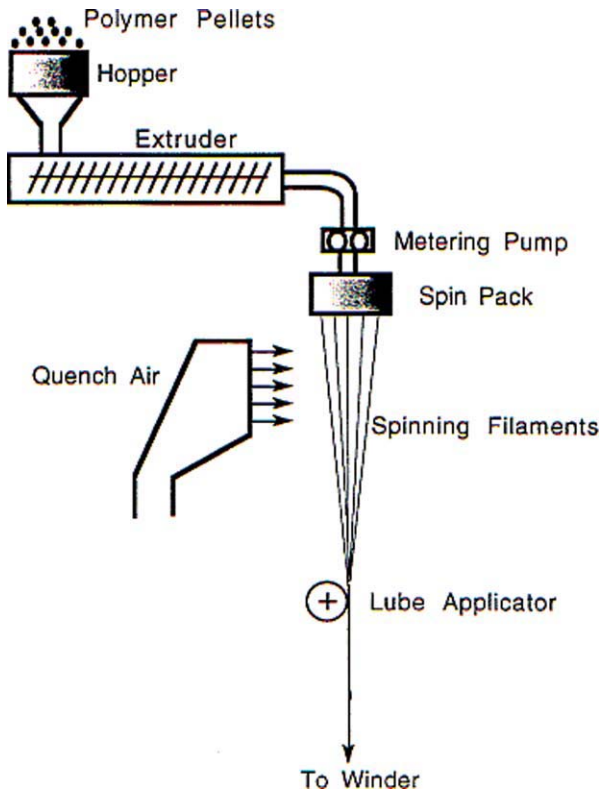

Figure 1 Schematic of the melt spinning line.

fibers. This article discusses the results of as-spun fiber studies. The findings of investigations pertaining to draw-annealing process will be continued in subsequent publications.

MATERIALS AND METHODS

Materials

Three variations of proprietary Fortron® linear PPS resins, varying in MW, in the pellets form were supplied by Ticona Polymers, a business of Celanese Chemicals. The sample codes are 1P, 2P, and 3P.

Polymer characterization

Melt flow index (MFI), of all three grades of polymers was determined using a Tinius Olsens' Extrusion Plastomer MP200. ASTM standard D1238[26] was followed for these measurements, with barrel temperature of 315°C and load of 5 kg as recommended for PPS.

Melting behavior of all three grades of PPS was studied using Mettler differential scanning calorimeter (DSC) 822^e. As-received pellets were dried under vacuum at 120°C for 3 hours prior to characterization. The rate of heating in DSC experiments was 10°C/min. After holding the melt at 325°C for 10 min, crystallization from melt was studied at a cooling rate of −10°C/min.

Melt spinning

Pilot melt spinning facility comprising of Fourne' single screw extruder was used. Freshly dried samples of each polymer were fed to feed hopper. Dry N_2 gas was continuously supplied to the hopper. The 12 holes spinnerets with 0.8 mm diameter capillary, and length to diameter (L/D) ratio of 10 and 5 were used to produce multifilament as-spun yarns. The filaments exiting the spinneret were allowed to cool under atmospheric conditions in around 2.5 m long spinline, and wound using a Leesona high speed winder. In the spinline, upon filament solidification, spin finish of 10% concentration (by volume), prepared in distilled water at room temperature, was applied to all the yarns under controlled rate so that spin finish pick up on the yarn was $\sim$ 1%. Figure 1[27] shows the schematic of the melt spinning line, and the spinning process parameters are given in Table I.

Fiber characterization

Fiber denier

Weight of 1 m length of the yarn, and the number of filaments in the yarn bundle were measured to calculate the filament denier. Denier is defined as the mass in grams of 9000 m length of the filament. For each sample, five readings were taken and the average is reported.

Tensile properties

The tensile properties of the as-spun fibers were measured using a Thwing-Albert tensile tester equipped with a 2000 g load cell. The testing was done on single filaments mounted on specially prepared paper tabs, to avoid fiber slippage in the jaws. For each sample, 10 single filaments taken from various portions of the yarn were glued on the tabs using epoxy resin and allowed to cure before testing. Gauge length (distance between the tab ends) used was 25.4 mm. Since as-spun fibers possessed larger extensions, the rate of extension for testing as-spun fibers was kept such that fibers broke in 20 ± 3 s as recommended in ASTM standard D3822.[28] Average of 10 readings is reported for tenacity and breaking elongation. Tenacity is defined as the breaking force per unit linear density, that is, denier. Tensile

TABLE I
Melt Spinning Process Parameters

Extrusion temperature (°C)	Throughput (g/12 holes/min)	Take-up speed (mpm)
Low (315) High (340)	Low (9) High (12)	Low (1025) Medium (1750) High (2350)

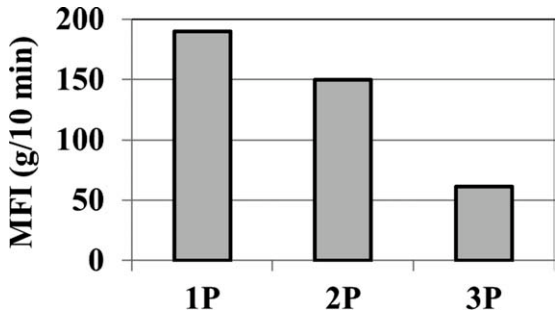

Figure 2 MFI of various PPS resins.

modulus was calculated from the load-elongation plots in the initial region of up to 2% elongation.

Morphological evaluations

Crystallinity

Degree of crystallinity (X) in fibers was evaluated using Mettler 822^e DSC. Prior to sample evaluations, DSC was calibrated using the standard indium and zinc samples. The yarn bundle was knotted carefully, without changing the sample history, to provide restraint in the easiest possible way during thermal analysis. Some kind of restraint was suggested by earlier researchers[29,30] to prevent any relaxation in fibers during heating in DSC. Around 4 mg of fibers was packed in the aluminum pan and heated to 325°C at 20°C/min under N_2 atmosphere. Degree of crystallinity was calculated using eq. (1).

$$X = \frac{\Delta H_f}{\Delta H_f^0} \tag{1}$$

where, ΔH_f is the heat of fusion of the sample determined from the DSC thermogram after subtracting the heat of crystallization, if any, that took place during heating. ΔH_f^0 is the heat of fusion of 100% crystalline PPS and was taken as 112 J/g.[31]

Molecular orientation

Overall orientation

Birefringence was measured using a polarized light optical microscope equipped with 20 order Ehringhaus compensator. To determine the extinction with more accuracy, monochromatic light filter of 587 nm was placed above the polarizer. From the average of three readings for each sample, measured (uncorrected) retardation (Γ_m) was noted from the retardation tables supplied by the compensator manufacturer.[32] To take into account the fringe jumping phenomenon that occurs in engineering polymers like PPS, corrected value of number of orders (N_d) was calculated using the method as described by Cha and Samuels.[33] To understand fringe jumping phenomena, readers may refer to the work of Faust and Marrinan.[34]

Crystalline orientation

Pin-hole patterns of parallel arrays of multifilament yarn laid on sample holder, were obtained using Molecular Metrology wide angle X-ray scattering (WAXS) system, on reusable Fuji image plates. X-rays of wavelength 1.5418 Å were produced using monochromatic CuKα radiation. It was operated at 45 kV and 0.66 mA, and the beam size was around 30 μm. The sample to film distance was set at 36.52 mm. Images obtained after enough sample exposure were subsequently read using the scanner, the FujiX-BAS 1800II image analyzer. Since the pin-hole patterns of as-spun fibers exhibited very little crystalline orientation, the plot of diffraction intensity of reflection from (110) plane as a function of azimuthal angle was constructed using the Polar software, to get an idea about the crystalline orientation in these fibers.

Dynamic thermomechanical analysis

Since, the as spun fibers were to be drawn subsequently at draw temperatures above glass transition temperature (T_g), thermomechanical response of as-spun fibers was evaluated using TA instruments' dynamic thermomechanical analyzer (DMA) series Q-800. The multifilament yarns of 8–10 mm length were subjected to constant tension of 0.05N at an oscillating frequency of 1 Hz. Temperature profile used was 25–200°C at the heating rate of 3°C/min.

Statistical analysis

The effect of several variables on as-spun fiber morphology and tensile properties was analyzed by constructing leverage plots using statistics software JMP 8.0. The correlation between the fiber morphology and properties was also evaluated statistically using this software. The solid line in leverage plots is the best fit based upon the data points, and dotted lines indicate 95% confidence limits.

RESULTS AND DISCUSSIONS

Polymer characteristics

MFI of PPS resins is shown in Figure 2. The order of MFI is 1P > 2P > 3P, and therefore, the order of MW can be deduced as 1P < 2P < 3P. MW of 3P is substantially higher than 2P, as compared to the difference in MW between 2P and 1P.

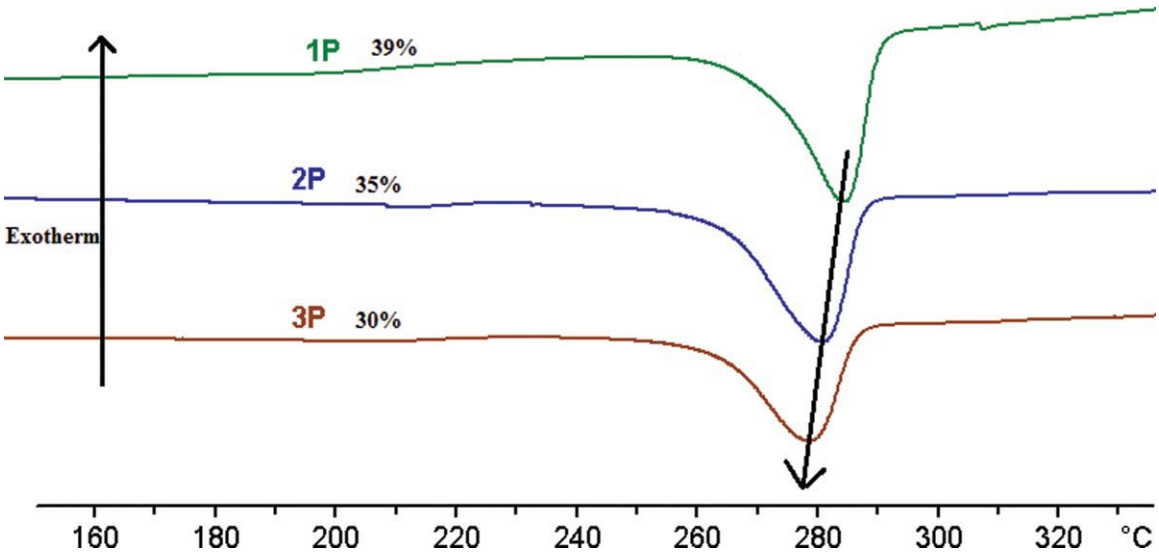

Figure 3 Melting behavior of PPS resins. [Color figure can be viewed in the online issue, which is available at wileyonlinelibrary.com.]

Thermal behavior of resins as studied by DSC is not significantly different (Fig. 3). Slightly lower peak melting temperature with increase in MW can be ascribed to the fact that with increase in MW, comparatively lower chain mobility due to more chain entanglements may lead to development of somewhat imperfect crystals. Similar dependence of peak melting temperature on crystals' nature was reported in other thermoplastic fibers, for example, polybutylene terephthalate.[35] The percentage value given above each of the thermograms in the figure is the degree of crystallinity developed in each of the polymers. With increase in MW, degree of crystallinity decreases. Similar MW dependence of degree of crystallinity in PPS has been reported earlier by other investigators.[4–10]

As-spun fiber structure and properties

In the following sections, the influence of several variables on as-spun fiber properties is discussed. Unless mentioned specifically, capillary L/D used was 10. Leverage plots are constructed using JMP 8.0 statistical software to understand the statistical significance of the effects. While plotting the effects of MW, inverse of MFI is taken so that the direct correlation with MW can be understood.

Fiber denier

Effect of take-up speed and throughput on denier of fibers spun from polymer 3P at two extrusion temperatures (ET) is shown in Figure 4. Fiber denier decreases with increase in take-up speed and decrease in throughput. At given process conditions, the draw-down ratio increases with increase in take-up speed, and with decrease in throughput. Increase in draw-down ratio leads to more drawing of the fibers and hence decreases the fiber denier. Similar behavior is observed in the fibers spun from 1P and 2P. Leverage plots revealed that the effect of take-up speed and throughput on fiber denier is highly statistically significant ($P < 0.0001$, where P is the probability of occurrence of the effect by chance).

Effect of polymer MW

Statistical significance of the influence of MW on fiber properties and morphology is shown in Figure 5. With increase in MW, tenacity increases [Fig. 5(a)] and breaking elongation decreases [Fig. 5(b)]. With increase in MW, the number of defects in the form of chain ends decreases, and chain entanglement increases. Therefore, due to

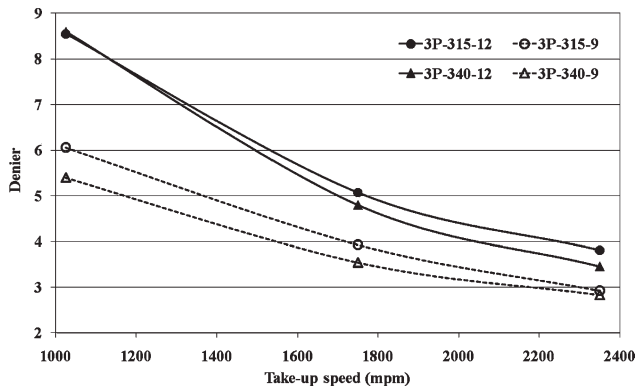

Figure 4 Factors influencing fiber denier. (Polymer 3P; throughput: solid lines-high and dotted lines-low; extrusion temperature: circle-low and triangle-high).

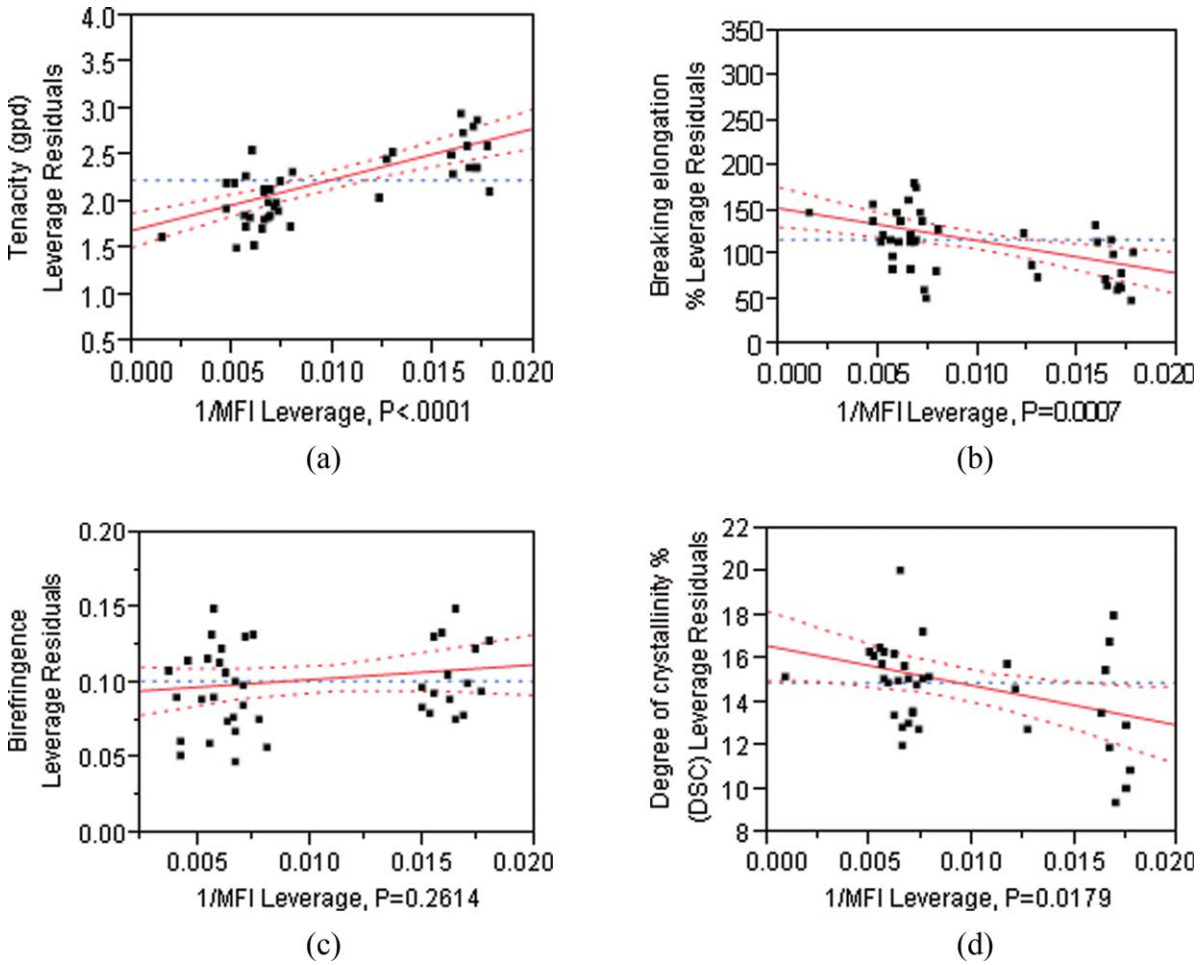

Figure 5 Leverage plots of effect of polymer MW (α 1/MFI) on (a) as-spun fiber tenacity; (b) breaking elongation; (c) birefringence; and (d) degree of crystallinity. (Samples matrix with all spinning process variables for three polymer types). [Color figure can be viewed in the online issue, which is available at wileyonlinelibrary.com.]

higher viscosity of the polymer at given extrusion temperature, melt of higher MW polymer experiences higher level of spinline stresses at given take-up speed. Resulting increase in molecular orientation as evidenced by increasing trend in birefringence [Fig. 5(c)] leads to increased fiber tenacity and decreased breaking elongation. Decrease in the level of crystallinity with increase in MW [Fig. 5(d)] can be explained on the basis that, with increase in MW molecular mobility decreases because of higher number of chain entanglements. In the spinline, within the short time available, before filament temperature drops to T_g due to rapid cooling, lower molecular mobility may be suppressing the crystallization more than the enhancement that may occur because of increase in spinline stress.

Tensile modulus of 3P fibers is found to be around 25 gpd (grams per denier) whereas that of 1P is found to be around 19 gpd. Higher tensile modulus of 3P fibers as compared to that of 1P can be attributed to higher molecular orientation in the former case.

Figure 6 shows the cold crystallization behavior of the as-spun fibers manufactured from all three resins spun under similar conditions. Higher the MW of

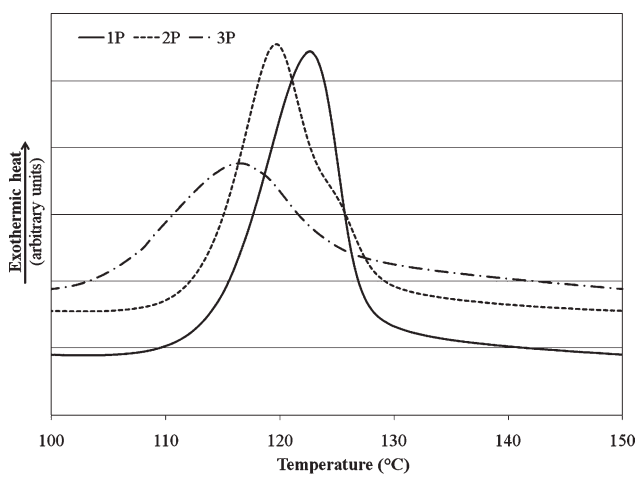

Figure 6 Influence of MW on cold crystallization behavior of as-spun fibers. (All fibers were spun at 1750 mpm; extrusion temperature 315°C; throughput: 12 g/min/12 holes).

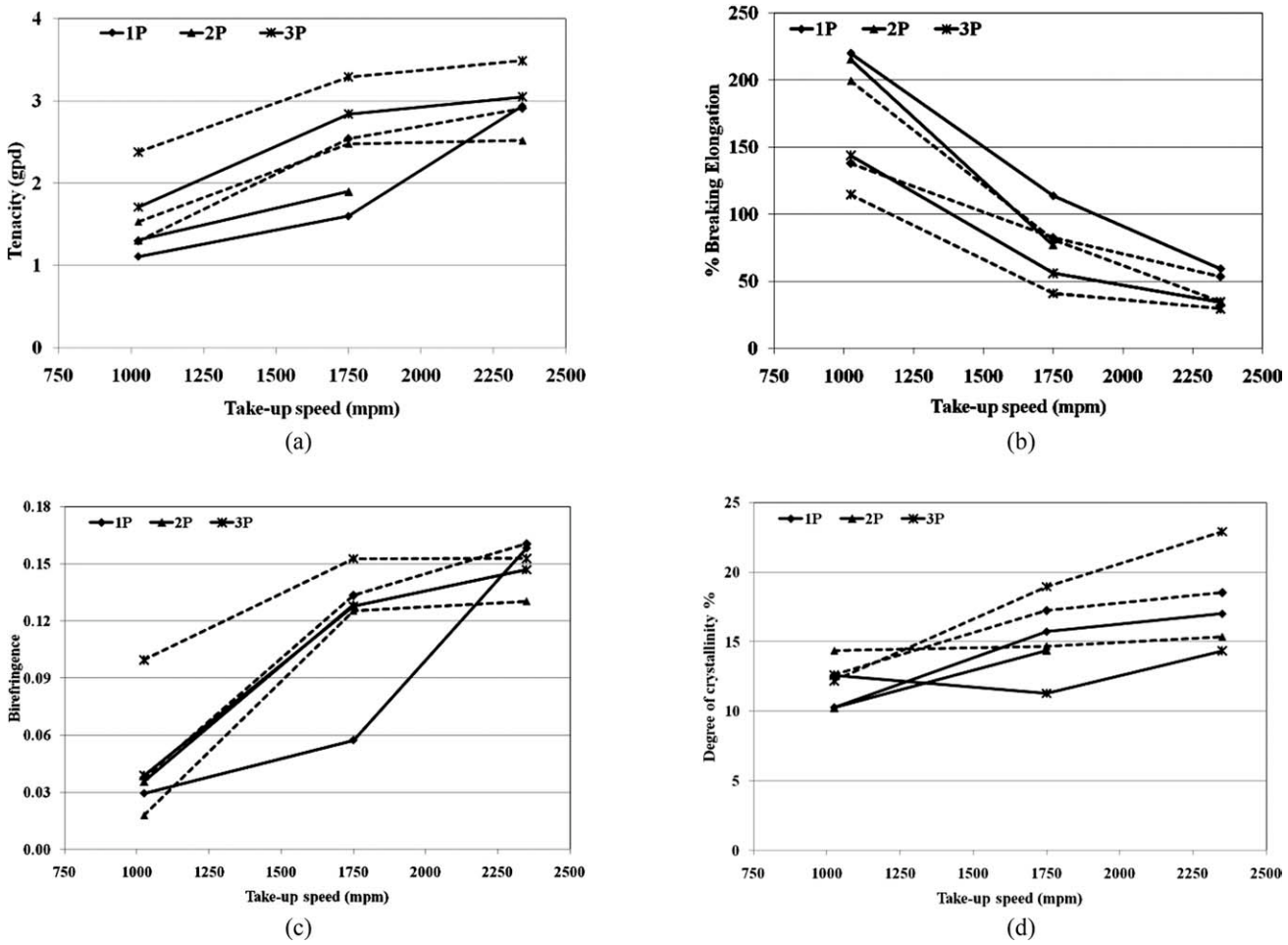

Figure 7 Effect of melt spinning variables on (a) as-spun fiber tenacity; (b) breaking elongation; (c) birefringence; and (d) degree of crystallinity. (Solid lines: high throughput; dotted lines: low throughput; extrusion temperature: 315°C, capillary L/D 10).

polymer from which fiber is spun, lower is the temperature of onset and peak in crystallization exotherm. It suggests that the higher the polymer MW, crystallization occurs earlier in the fibers. When spun under similar processing conditions, the spinline stress, and therefore, molecular orientation will be higher in fibers spun from high MW polymers as discussed before. In the presence of chain mobility induced thermally above T_g during DSC experiments, the fiber structure with higher orientation is more favorable for crystallization, and hence the fiber crystallizes earlier.

Effect of take-up speed

Effect of take-up speed and throughput on as-spun fiber tensile properties is shown in Figure 7, and the corresponding leverage plots are shown in Figure 8. With increase in take-up speed, tenacity [Figs. 7(a) and 8(a)], birefringence [Figs. 7(c) and 8(c)], and degree of crystallinity [Figs. 7(d) and 8(d)] increase, and breaking elongation decreases [Figs. 7(b) and 8(b)]. At higher take-up speeds, higher spinline stresses exerted on the filaments lead to improvement in the molecular orientation along the fiber axis and improved molecular orientation, as seen by increase in birefringence results in increase in tenacity and decrease in elongation. Besides its dependence on time and temperature, crystallization is influenced by stresses as well. The time available for crystallization before fiber temperature drops below T_g may not be significantly different at various take-up speeds. Under these circumstances, for a given polymer, increasing spinline stress with increase in take-up speed causes the degree of crystallinity to increase due to stress induced crystallization. It is to be noted that even at highest take-up speed studied; the degree of crystallinity is lower (close to 20%) than crystallization potential ($\sim$ 30–35%) of these polymers under quiescent conditions as discussed earlier. Slow increase in crystallinity with take-up speed up to 4000 mpm was reported by Chen et al.[36] in the case of PET melt spun fibers.

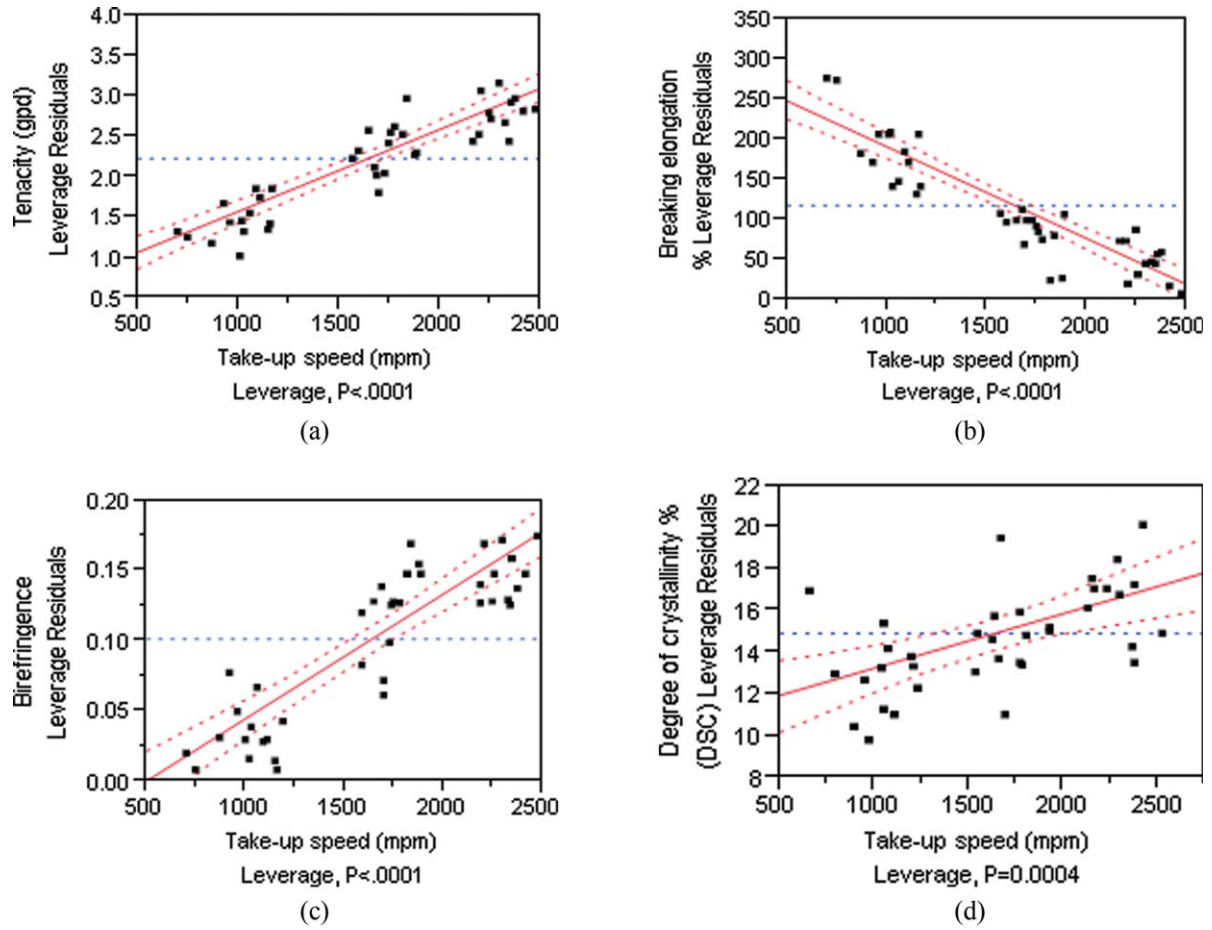

Figure 8 Leverage plots of effect of take-up speed on (a) as-spun fiber tenacity; (b) breaking elongation; (c) birefringence; and (d) degree of crystallinity (sample matrix of all other process parameters combined). [Color figure can be viewed in the online issue, which is available at wileyonlinelibrary.com.]

Trends in Figure 7 indicate that the rate of change in fiber properties is higher initially, and decreases thereafter with increase in take-up speed. It implies that the amount of change brought by the take-up speed in fiber properties is not linear but rather decreases with increase in speed. Similar observations were reported in the case of fibers spun from isotactic polypropylene[37] and from PET.[38] Ziabicki[39] explained this phenomenon on the basis of the competition between crystallization and rapid cooling, during fiber spinning. With increase in take-up speed, rate of crystallization increases due to higher

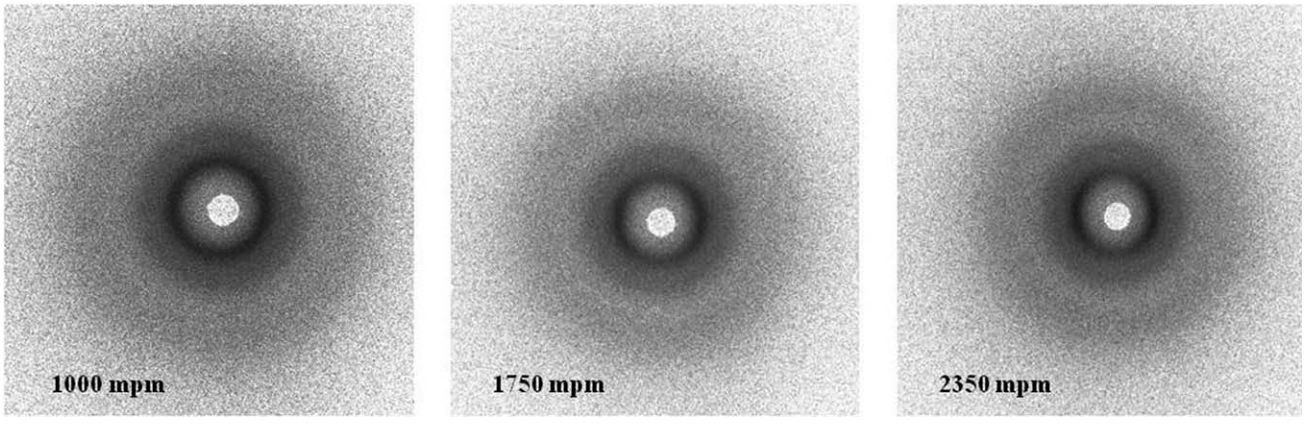

Figure 9 WAXS pin-hole patterns (fiber axis vertical). (Fiber spinning conditions: Polymer: 3P; extrusion temperature: 315°C; throughput: 12 g/min/12 holes; capillary L/D: 10).

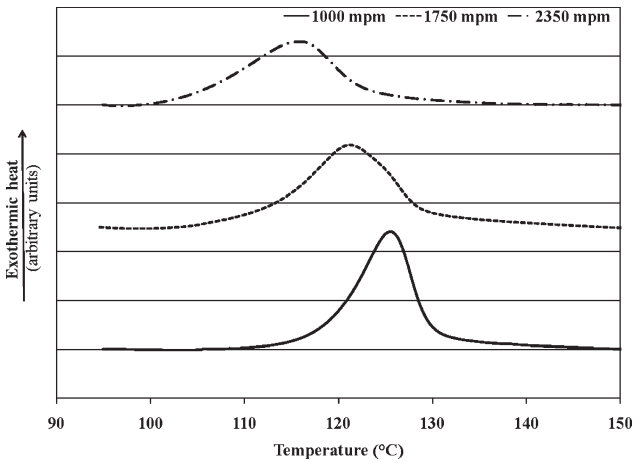

Figure 10 DSC thermogram (heating curves) of as-spun fibers spun at different take-up speeds. Values of crystallinity are above each curve.

spinline stresses. Conversely, the time available for crystallization decreases due to faster cooling of finer filaments with take-up speed increase. Thus the product of the available time for crystallization and crystallization rate reaches maximum at critical take-up speed and decreases thereafter. This phenomenon seems to be valid in the case of PPS as well.

Enhancement in fiber morphology is further substantiated by studying crystalline structure development in as-spun fibers using WAXS. WAXS pin-hole patterns of as-spun fibers prepared from 3P at different take-up speeds are shown in Figure 9. At a take-up speed of 1000 mpm, very little crystallinity with negligible crystalline orientation is developed in the fiber. In the absence of separate reflections corresponding to different crystal planes, quantitative evaluation of crystalline orientation was not possible. With increase in take-up speed, appearance of arcs indicates slight increase in crystalline orientation. Similar observations were made in the case of fibers manufactured from other polymers including PPS by several investigators.[20,40,41].

Figure 10 shows the effect of take-up speed on cold crystallization behavior of as-spun fibers

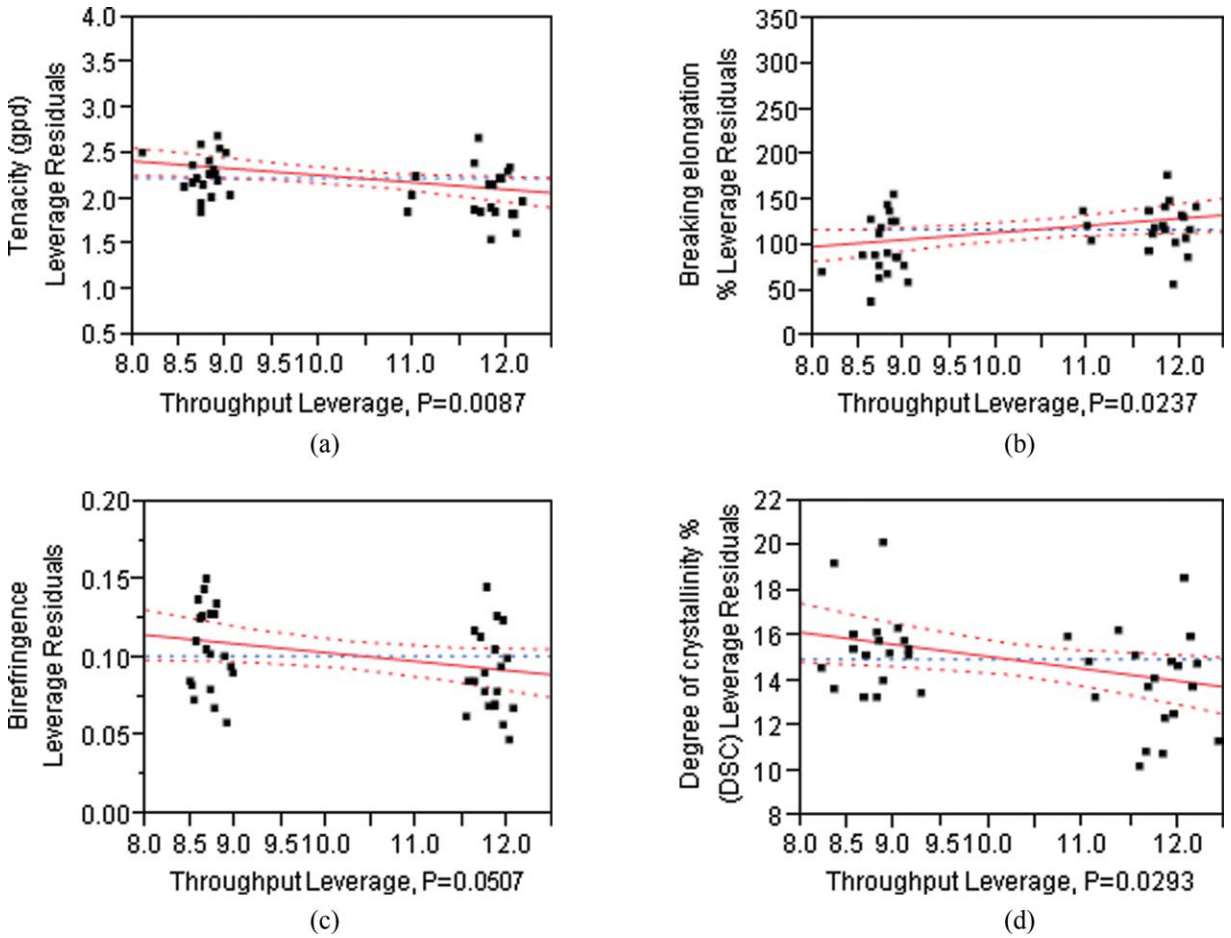

Figure 11 Effect of throughput on (a) as-spun fiber tenacity; (b) breaking elongation; (c) birefringence; and (d) degree of crystallinity (all other process variables combined). [Color figure can be viewed in the online issue, which is available at wileyonlinelibrary.com.]

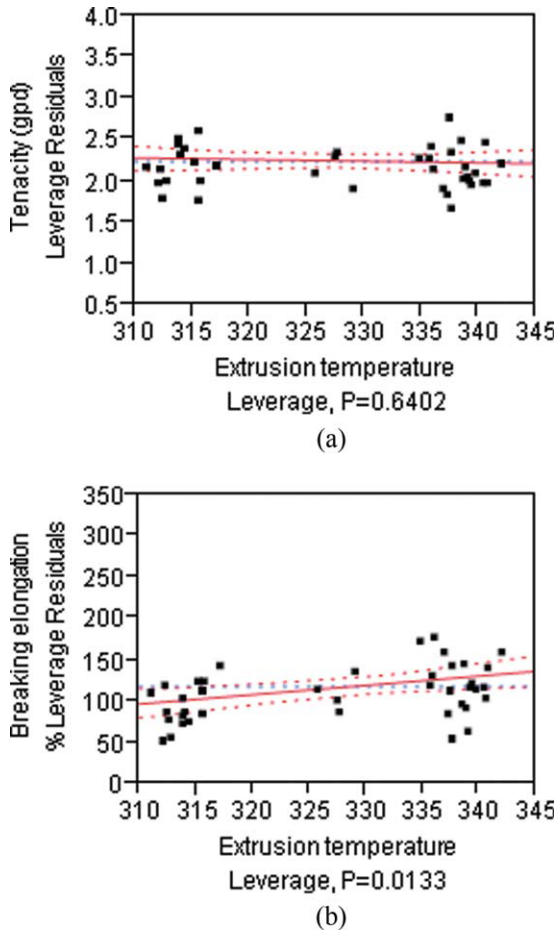

Figure 12 Effect of extrusion temperature on (a) as-spun fiber tenacity; (b) breaking elongation (all other process variables combined). [Color figure can be viewed in the online issue, which is available at wileyonlinelibrary.com.]

manufactured from polymer 3P at ET of 340°C and high level of throughput. The percentages adjacent to each of the thermograms indicate the degree of crystallinity developed in the fibers during heating. When manufactured from same polymer at similar level of throughputs, fibers spun at higher take-up speeds crystallize earlier. As discussed before, this behavior can also be supported by the development of spinline stresses as a function of take-up speed. The fibers spun at higher take-up speeds exhibit lesser crystallinity development during heating due to the fact that these fibers possess higher degree of crystallinity to begin with.

Effect of throughput

With increase in throughput, changes in fiber properties follow similar trends as observed with decrease in take-up speed. Figure 11 shows the leverage plots for this variable whereas actual data of fiber properties versus throughput was shown earlier in Figure 7. Decrease in draw-down ratio with increase in throughput lowers the spinline stresses on fibers. This explains observed decrease in birefringence [Fig. 11(c)] and degree of crystallinity with increase in throughput [Fig. 11(d)]. Decrease in molecular orientation and crystallinity results in decrease in tenacity [Fig. 11(a)] and increase in breaking elongation [Fig. 11(b)].

Effect of extrusion temperature

Within the range of temperatures studied, ET exhibits negligible influence on the fiber properties with certain trend. With increase in ET, slight decrease in tenacity and increase in breaking elongation (Fig. 12) may be explained by the fact that with increase in ET, melt viscosity decreases. Therefore, melt experiences lower levels of shear stresses and spinline stresses within the die and upon exiting the spinneret respectively. Both these factors may cause lower level of molecular orientation of molecular chains along the fiber axis, and result in slight decrease in the fiber tenacity at higher ET. Decrease

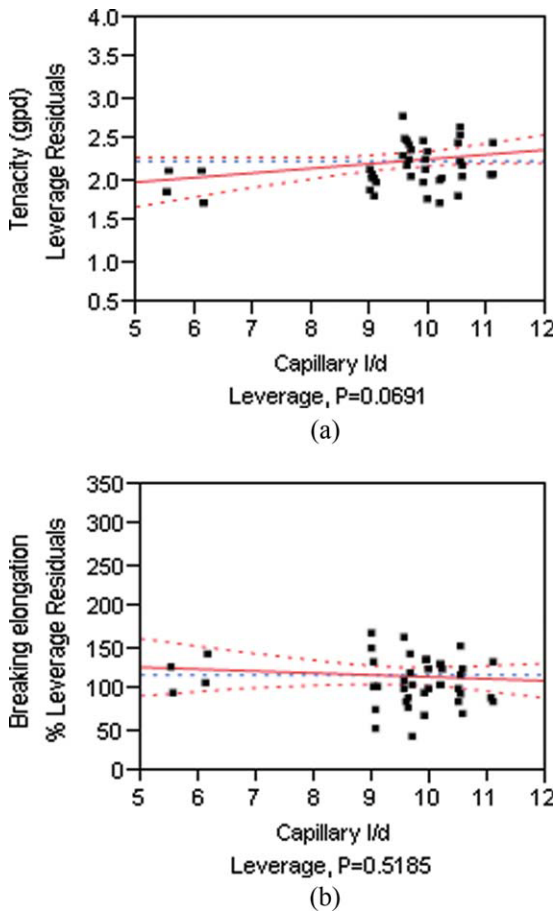

Figure 13 Effect of capillary L/D on (a) as-spun fiber tenacity; (b) breaking elongation (all other process variables combined). [Color figure can be viewed in the online issue, which is available at wileyonlinelibrary.com.]

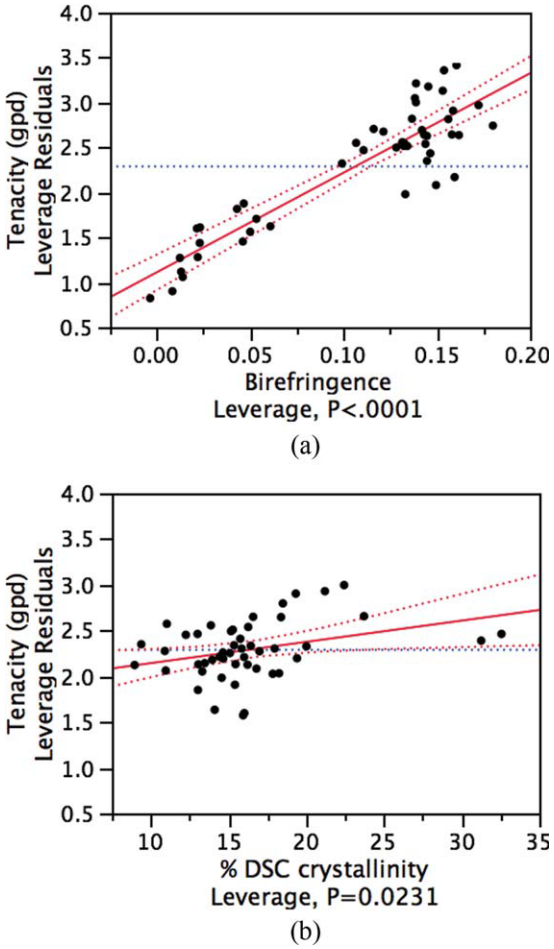

Figure 14 Dependence of fiber tenacity on (a) birefringence and (b) % DSC crystallinity. [Color figure can be viewed in the online issue, which is available at wileyonlinelibrary.com.]

in tenacity with increase in ET was reported by Chen et al.[36] in PET melt spun fibers.

Effect of capillary L/D

With increase in capillary L/D from 5 to 10, increase in fiber tenacity [Fig. 13(a)] and decrease in breaking elongation [Fig. 13(b)] are observed. However, within the range of capillary L/Ds studied, the effect is not statistically significant. With increase in capillary L/D, the time available for the melt to flow through capillary increases, giving more time for the chains to orient in the direction of flow in the presence of shear stresses within the channel. Therefore, within the capillary, elastic part of the energy will be lesser with longer capillaries, resulting into lower die swell. Correspondingly, lower loss of the molecular orientation occurs upon capillary exit. Higher level of molecular orientation retained in the fiber structure thereby leads to increase in tenacity and decrease in breaking elongation.

Structure-properties correlation in as-spun fibers

The strong positive correlation between as-spun fiber tenacity and birefringence is shown in Figure 14(a), indicating that with increase in molecular orientation along the fiber axis, fiber tenacity increases. Also shown is the statistically significant positive correlation of tenacity with crystallinity in Figure 14(b), although the *P* value is somewhat higher for tenacity-crystallinity relationship as compared to that for tenacity-birefringence relationship.

To understand the effectiveness of material and process variables to predict the as-spun fiber properties, regression plots of actual versus predicted properties are shown in Figure 15 for tenacity and birefringence. *R*-square (RSq) value of more than 0.80 suggest that the fiber properties, that is, tenacity and birefringence are well explained on the basis of variables that include polymer MW and melt spinning process parameters, that is, ET, throughput and take-up speed.

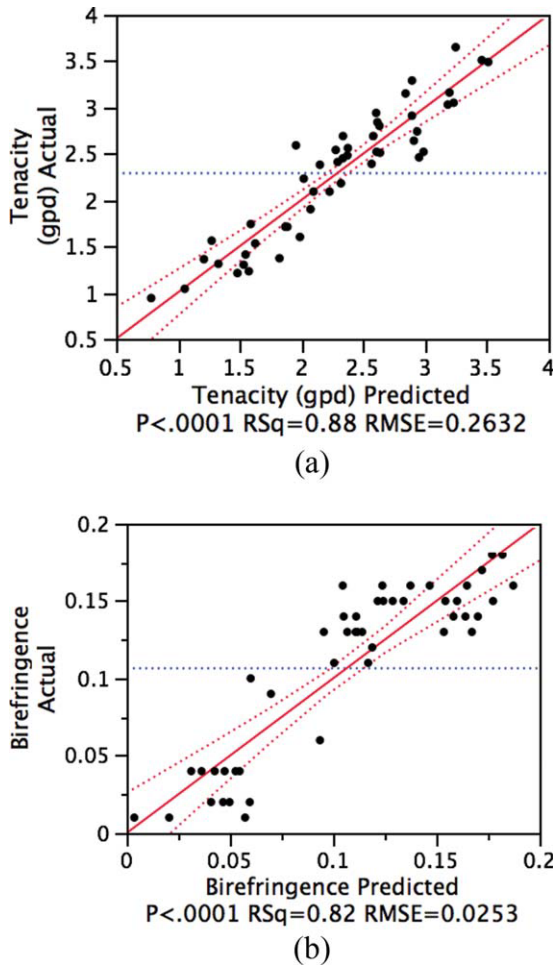

Figure 15 Actual versus predicted fiber properties (a) tenacity and (b) birefringence. [Color figure can be viewed in the online issue, which is available at wileyonlinelibrary.com.]

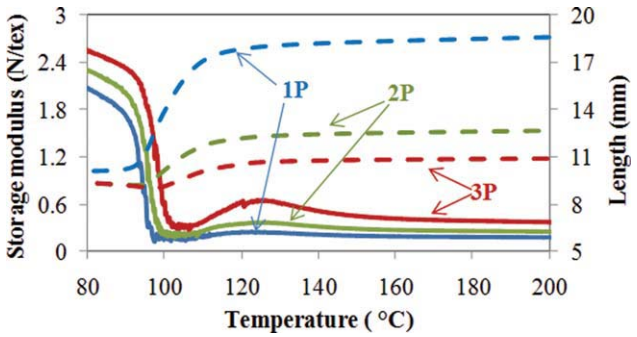

Figure 16 Dynamic mechanical behavior of as-spun fibers: solid lines, storage modulus, dotted lines, length. (As-spun fibers spun at 1750 mpm, extrusion temperature: 315°C, throughput: 12 g/min/12 holes, capillary l/day 10). [Color figure can be viewed in the online issue, which is available at wileyonlinelibrary.com.]

Dynamic mechanical behavior of as-spun fibers

Changes in storage modulus and in length of as-spun fibers recorded during DMA tests are shown in Figure 16. These fibers were manufactured from all three polymers under similar spinning process conditions. It is clear from Figure 16 that with higher polymer MW, the minimum in storage modulus occurs at higher temperature. Corresponding change in length is also shown on secondary axis in Figure 16. Above $T_{g,}$ as-spun fibers of 1P show viscous flow like behavior without any shrinkage. Comparatively, fibers spun from 2P and 3P shrink increasingly in the order of their MW, before exhibiting the viscous flow like behavior. It is further noted that the temperature at which viscous flow begins increases as the polymer MW increases. Prior to the onset of viscous flow, increasing amount of shrinkage above T_g in the as spun fibers with increasing polymer MW, indicates presence of higher level of stresses and therefore molecular orientation due to increasing number of chain entanglements. Higher level of molecular orientation is supported by higher birefringence in 3P fiber (0.128) than in 1P fiber (0.057). Similar behavior was observed during DMA testing of fibers spun from 1P at take-up speeds of 1750 mpm and 2350 mpm. The fibers spun at 2350 mpm showed minimum storage modulus and onset of viscous flow at higher temperature than the fiber spun at 1750 mpm. Also former showed shrinkage before the onset of viscous flow. Birefringence of 1P fiber spun at 1750 mpm was 0.057, and that of the fiber spun at 2350 mpm was 0.158. Thus, higher level of molecular orientation at higher take-up speeds can be attributed to observed dynamic mechanical behavior of the as-spun fibers.

In a study on heat treatment of PET fibers, Peszkin and Schultz[42] reported that the physical crosslinks are necessary to produce shrinkage during heating the fibers by preventing free movement of chain through each other. In the absence of physical crosslinks in the form of chain entanglements, crystallites, oriented chains, etc., due to either lower MW or lower take-up speed during melt spinning, viscous flow in present experiment suggests that the chain mobility induced at higher temperatures may result in chains sliding past each other without appreciable resistance. Thus from the trends in Figure 16, it can be stated that with increase in stress level in the as-spun fibers, either by increase of MW or by spinning at higher take-up speeds, the viscous flow like behavior and the failure to stretch the fibers due to chain sliding past each other shifts to higher temperature. This important observation may have a significant bearing during drawing of these fibers.

CONCLUSIONS

The structure-properties development in the as-spun PPS fibers indicates that the fiber tenacity increases and elongation decreases with increase in polymer MW, with increase in take-up speed, and with decrease in throughput. Within the range of temperatures studied, extrusion temperature exhibits negligible influence on as-spun fiber properties. The most significant variables affecting fiber properties are found to be polymer MW, take-up speed and throughput. As-spun fibers with tenacities close to 4 gpd and breaking elongations around 30% were obtained by spinning at high take up speeds. The degree of crystallinity developed in the as-spun fibers as a function of spinning process variables varied in the range of 10–20%. As-spun fiber tenacity is positively correlated with birefringence and the differences are statistically significant. The molecular orientation enhances the crystallization behavior in fibers. The thermomechanical behavior of as-spun fibers shows a definite trend and is influenced by physical crosslinks.

We sincerely thank Ticona Polymers for supplying various grades of proprietary Fortron® linear PPS resins used. Continued interaction with Dr. Manoj Ajbani, Dr. Ke Feng, and Lisa Baker (all from Ticona Polymers) is gratefully acknowledged. The financial support from Center for Materials Processing, The University of Tennessee, Knoxville during the studies of PG is also highly acknowledged.

References

1. Edmonds, J. J. T.; Hill, J. H. W. (Phillips Petroleum Company). U.S. Pat.3,354,129 (1967).
2. Lenz, R. W.; Carrington, W. K. J Polym Sci 1959, 41, 333.
3. Lenz, R. W.; Handlovits, C. E. J Polym Sci 1960, 43, 167.
4. Jog, J. P.; Nadkarni, V. M. J Appl Polym Sci 1985, 30, 997.
5. Menczel, J. D.; Collins, G. L. Polym Eng Sci 1992, 32, 1264.
6. Lovinger, A. J.; Davies, D. D.; Padden, F. J Polym 1985, 26, 1595.
7. Lopez, L. C.; Wilkes, G. L. Polymer 1988, 29, 106.
8. Lopez, L. C.; Wilkes, G. L. Polymer 1989, 30, 882.

9. Chung, J. S.; Cebe, P. J. J Polym Sci Part B: Polym Phys 1992, 30, 163.
10. Collins, G.; Menczel, J. Polym Eng Sci 2004, 32, 1270.
11. Hawkins, R. T. Macromolecules 1976, 9, 189.
12. Scobbo, J. J., Jr. J Appl Polym Sci 1993, 48 2055.
13. Scobbo, J. J., Jr. J Appl Polym Sci 1993, 47, 2169.
14. Lopez, L. C.; Wilkes, G. L. J Macromol Sci. Rev in Macromol Chem Phys 1989, 29, 83.
15. Brady, D. G. J Appl Polym Sci 1976, 20, 2541.
16. Christopher, N. S. J.; Cotter, J. L.; Knight, G. J.; Wright, W. W. J Appl Polym Sci 1968, 12, 863.
17. Jog, J. P.; Bulakh, N.; Nadkarni, V. M. Bull Mater Sci 1994, 17, 1079.
18. Budgell, D. R.; Day, M. Polym Eng Sci 1991, 31, 1271.
19. Zhang, R.-C.; Xu, Y.; Lu, A.; Cheng, K.; Huang, Y.; Li, Z. M. Polymer 2008, 49, 2604.
20. Song, S. S.; White, J. L.; Cakmak, M. Int Polym Process 1989, 2, 96.
21. Carr, P. L.; Ward, I. M. Polymer 1987, 28 2070.
22. Krins, B.; Feijen, H. H. W.; Heuzeveldt, P.; Vieth, C. R. E. (Diolen Industrial Fibers Bv) Neth. Can. Pat. 2,601,751 (2006).
23. Murthy, N. S.; Elsenbaumer, R. L.; Frommer, J. E.; Baughman, R H. Synth Met 1984, 9, 91.
24. Suzuki, A.; Kohno, T.; Kunugi, T. J Polym Sci Part B: Polym Phys 1998, 36, 1731.
25. White, J L.; Dharod, K. C.; Clark, E. S. J Appl Polym Sci 1974, 18, 2539.
26. ASTM D1238-04C, Standard test method for melt flow rates of thermoplastics by extrusion plastometer.
27. Spruiell, J. E. In Structure formation in polymeric fibers; Salem, D., Ed.; Hanser Gardener Publications Inc., Cincinnati 2000, p 5–93.
28. ASTM D3822, Standard test method for tensile properties of single textile fibers 2007.
29. Jaffe, M. In Thermal Characterization of Polymeric Materials; Turi, E. A., Ed.; Academic Press: Orlando Florida, 1981, p 709–792.
30. Todoki, M.; Kawaguchi, T. J Polym Sci Part B: Polym Phys 1977, 15, 1507.
31. Huo, P.; Cebe, P. Colloid Polym Sci 1992, 270, 840.
32. Data from manufacturer, Ehringhaus compensator.
33. Cha, C. Y.; Samuels, R. J. J Polym Sci Part B: Polym Phys 1995, 33, 259.
34. Faust, R. C.; Marrinan, H. J. Br J Appl Phys 1955, 6, 351.
35. Chen, S.; Spruiell, J. E. J Appl Polym Sci 1987, 33, 1427.
36. Chen, G. Y.; Cuculo, J. A.; Tucker, P. A. J Appl Polym Sci 1992, 44, 447.
37. Shimizu, J.; Okui, N.; Kikutani, T. Sen-i-Gakkaishi 1979, 35, T-405.
38. Vassilatos, G.; Knox, B. H.; Frankfort, H. R. E. In High speed fiber spinning; Ziabicki, A., Kawai, H., Eds.; Wiley: New York, Chapter 14, 1985.
39. Ziabicki, A. Fiber world 1984, 1, 8.
40. Spruiell, J. E.; White, J. L. Polym Eng Sci 1975, 15, 660.
41. Ziabicki, A.; Jarecki, L. In High Speed Fiber Spinning-Science and Engineering aspects; Ziabicki, A., Kawai, H., Eds.; Wiley: New York, 1985, p 225.
42. Peszkin, P. N.; Schultz, J. M. J Appl Polym Sci 1985, 30, 2689.